Journal of Materials Processing Technology 168 (2005) 327–335

Journal of Materials Processing Technology

www.elsevier.com/locate/jmatprotec

Finite element bending analysis of oval tubes using rotary draw bender for hydroforming applications

Hokook Lee [a], C.J. Van Tyne [b,*], David Field [c]

[a] *Division of Engineering, Colorado School of Mines, Golden, CO 80401, USA*
[b] *Department of Metallurgical and Materials Engineering, Colorado School of Mines, Golden, CO 80401, USA*
[c] *Research & Development Center, General Motors Corporation, Warren, MI 48090, USA*

Received 1 April 2004; received in revised form 1 November 2004; accepted 1 November 2004

Abstract

In manufacturing automotive parts, such as engine cradles, frame rails, subframes, cross-members, and other parts from circular tubes, pre-bending and pre-forming operations are often required prior to the subsequent tubular hydroforming process. During some pre-forming operations, the cross section of a bent circular tube is crushed into an oval-like shape to ensure proper geometry and sufficient clearance in the hydroforming dies. For such applications, the use of oval instead of circular tubes could be an effective means of eliminating the pre-forming step. The oval tube could also be produced with less thinning and with less strain on the outside of the bend when controlled by a booster system without the use of mandrel. Oval tubes may also reduce manufacturing expenses by reduced labor and pre-forming equipment costs. Hence, the understanding of the issues that occur in the bending of oval tubes is worthy of investigation. This paper presents detailed parametric studies on the bending of oval tubes without a mandrel. The finite element modeling technique is used to examine the deformation characteristics such as wall thinning, strain, side-bulge, flattening, and hoop-buckle for both circular and oval tubes. In the simulations, the bending process parameters of bend radius, aspect ratio of the tube ovalness, and tube wall thickness are varied. Observations are made to obtain a hoop-buckle limit diagram in terms of a non-dimensionalized shape degradation factor. Suggestions based upon developed criteria are made on the acceptability of bent tubes suitable for hydroforming applications without the need of a pre-forming step or the use of a mandrel.

Keywords: Tubular hydroforming; Rotary draw bending; Oval tubes; Finite element modeling; Hoop-buckle limit diagram; Shape degradation factor; Acceptability conditions

1. Introduction

Recently, the use of tubular hydroforming technology has seen increased usage and increased consideration for various tubular automotive applications, such as exhaust manifolds, chassis components, engine and power train components, and body and safety components [1]. Although the hydroforming technique has some drawbacks, including relatively slow production rates, heavy initial investment in equipment, and small knowledge-base for the process and tool design, it has been successfully implemented in a variety of the applications with many advantages such as better structural integrity of product, reduced weight and manufacturing cost, material saving, improved structural reliability and dimensional tolerances, and fewer secondary operations [1,2]. Three production steps are usually carried out to produce a tubular hydroformed part—roll-forming, pre-forming such as tube bending, and hydroforming. As the material goes through these steps, it is deformed along complicated strain-paths with increases in the strength of the material due to strain hardening. Typical values of the strain in “aluminum killed draw quality” (AKDQ) steel for each step are as follows: 5–15% for roll-forming, 20–30% for tube bending, and 5–15% for hydroforming [3]. During the bending operation, most of the strain takes place in the material. Thinning on the outside of the bend approaches approximately 20% for the minimum recommended bend ra-

* Corresponding author. Tel.: +1 303 273 3793; fax: +1 303 273 3795.
E-mail address: cvantyne@mines.edu (C.J.Van Tyne).

0924-0136/$ – see front matter © 2005 Elsevier B.V. All rights reserved.
doi:10.1016/j.jmatprotec.2004.11.019

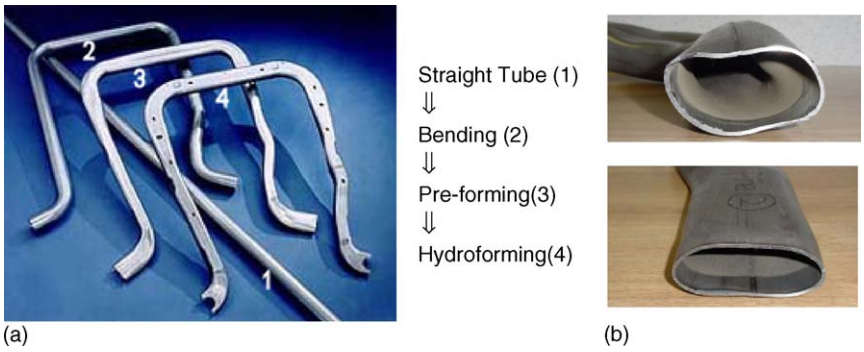

Fig. 1. (a) Typical production steps for an engine cradle (Schuler Hydroforming Inc.), and (b) cross-sectional shapes after the pre-forming.

dius of two times the tube diameter. Thinning of 33% occurs for bending with a bend radius equal to the tube diameter [3]. The bending formability depends on geometric factors, the tool set, and the booster system. The dominant bending parameters should be precisely controlled to minimize the excessive thinning and strain on the outside of the bend.

There have been a number of studies investigating the hydroforming process. Most have focused on precise control of forming parameters such as die closing, internal pressure, and axial feeding. However, the significance of the bending operation, which is often performed prior to the hydroforming operation, has received less attention. Large localized changes in the strain and the thinning on the outside of the bend occur during the bending. The strain and thinning from bending can affect the potential for success of the subsequent hydroforming operation. To date, only a few studies on tube bending have been undertaken for hydroforming applications, and most of them have examined bending characteristics of circular tubes. For example, thickness changes with or without a mandrel [3], contribution of a booster system on tube rotary draw bending for ferritic (F12T, F17TNb) and austenitic (18-9D, 18-10T) stainless steel tubes [4], pre-bending simulations to examine the effect of bending parameters on shape and thickness changes of cross-sections [5], review of bender types, simplified analytical models and some bending simulations compared with experimental measurements [6], effect of pressure acting on the clamp die, pressure die and booster, booster speed, bending speed, and on changes in the thickness and degree of flatness for A6063 aluminum tubes [7] have all been investigated.

Bending of round tubes in various planes is often used in the automotive industry. Due to cost reduction pressures, the use of oval tubes has rarely been implemented in automotive manufacturing and the single production use of oval tubes had bends in only a single plane. One tube bending machine for oval tubes was built where bending occurred in two planes defined by the centerline of the tube and the major and minor axes of the cross section. The machine was never put into production. In spite of these past limitations, the examination of oval tube bending is worthy of study because of unique capabilities that it can provide.

In order to manufacture automotive parts such as engine cradles, frame rails, subframes, cross-members, and other candidate parts from circular tubes, pre-bending and pre-forming operations are often required prior to the tubular hydroforming process. Fig. 1 shows (a) the typical production steps of an engine cradle and (b) the cross-sectional shapes of the tube after the part has been preformed. During the pre-forming operation, the cross-section of a bent circular tube is crushed into an oval-like shape, so that proper geometry and sufficient clearance in the hydroforming dies can be ensured to avoid pinching when the top die is brought down to the closed position. The pre-forming steps also produce flat areas on the tube for subsequent attach points used to mate with other components during subsequent assembly. For such applications, the use of oval tubes instead of the circular tubes could be an effective means of eliminating a pre-forming step. It could also produce less thinning and strain on the outside of the bend when controlled by a booster system without engaging a mandrel. The use of oval tubes may also reduce manufacturing cost through labor savings and the reduced need for pre-forming equipment. Therefore, understanding the issues that occur in the bending of oval tubes is worthwhile, since it may become a viable fabrication route for certain components.

In this paper, detailed parametric studies are presented on the bending of oval tubes without a mandrel. The finite element modeling technique is used to study deformation characteristics, such as wall thinning, strain, side-bulge, flattening and hoop-buckling for circular and oval tubes. The simulations examine various process parameters, such as bend radius, geometrical aspect ratio of the oval tube, and wall thickness. Observations are made to obtain a hoop-buckle limit diagram, as well as to suggest acceptability conditions for bending a tube, which would be suitable for a tubular hydroforming application without the need of a pre-forming step.

2. Finite element modeling

Tube bending is a forming process in which a straight piece of tube is deformed to a selected bend radius and bend angle.

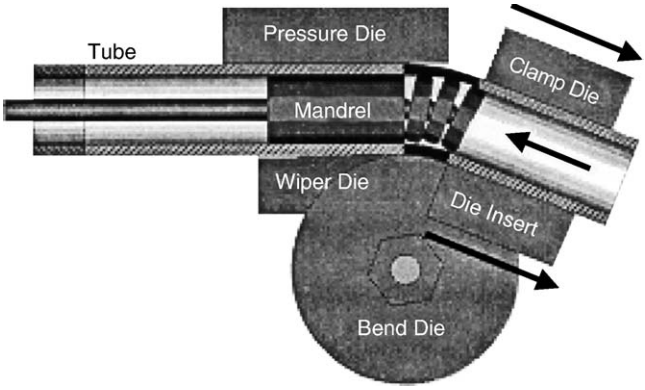

Fig. 2. Schematic of rotary draw bender (Eagle Precision Technologies Inc.).

Tube bending can be done using several different methods, such as ram bending, press bending, roll bending, and rotary draw bending [8]. Among these methods, the rotary draw bending method (shown in Fig. 2) is the most versatile, cost-effective, and precise method for tight bending radii and thin walled tubes [9].

Computer simulations using the finite element method to predict the structural performance are widely used in the automotive industry, and provide designers with an effective means of building confidence into products and tool designs. The finite element modeling on the tube bending process is capable of accurately representing the following factors: tool and die geometries, boundary constraints, surface interactions, and material properties in the forming range. In this study, a commercially available implicit finite element code, MARC, is used to predict the bending behaviors of oval tubes. A user-developed program, virtual rotary draw bender (VRDB) was developed to automatically generate the finite element bending models for the pre- and post-processor, MENTAT, and was used to interpret the simulation results with customized visualizations. Table 1 lists the values for the process parameters used in the FEM simulations, where R_b is the bend radius, γ the aspect ratio (ratio of length of the minor axis to the major axis on the oval cross section), and t_o is the wall thickness. For each simulation, the following common conditions were used: length of the major axis of 70.0 mm, bending speed of $\pi/4$ rad/s, and total bend-angle of 90°. A mandrel was not used. Hard-way bending, in which the major axis of the oval cross section is parallel to the plane of the bend, was carried out in all simulations. Additionally, a Coulomb friction model with 0.1 friction coefficient was implemented to mathematically represent the friction behavior along all tube–tool interfaces.

Table 1
Process parameters for FEM simulations with fixed major axis of 70 mm

Bend radius, R_b (mm)	Aspect ratio, γ	Wall thickness, t_o (mm)
	0.3	1.0
70.0	0.5	1.5
105.0	0.6	2.0
140.0	0.7	2.5
175.0	0.8	3.0
210.0	1.0	3.5

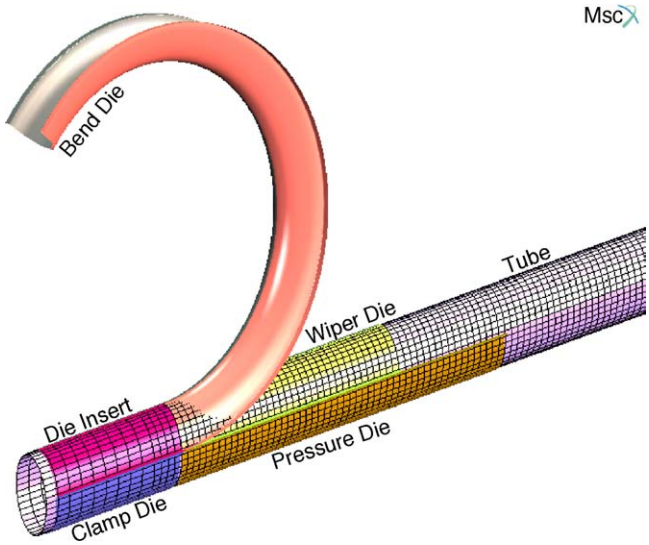

Fig. 3. A representative finite element model for the bending simulation of an oval tube (R_b = 175.0 mm, γ = 0.5 and t_o = 2.0 mm).

Fig. 3 shows a representative finite element model with the initial tubular blank and tool set. The tools and tubular blank were modeled with the half geometry due to symmetry. All tools were represented as rigid bodies, and the groove profiles that contact the tubular blank were modeled based on the given aspect ratio. Four-node shell elements with seven layers comprised the tubular blank. An isotropic, homogeneous, elastic–plastic material following the Von-Mises yield criterion, with isotropic work hardening, was the material model.

To obtain the mechanical properties of the steel tube an expansion test of a straight tube was performed. The stress was derived from pressure and the instantaneous geometry of the tube, assuming homogeneous deformation and no anisotropy. The strains were determined from strain gauges directly attached to the tube during the test. The constitutive equation representing the material behavior was obtained through the Marquardt's curve fitting method [10]. Fig. 4 shows the

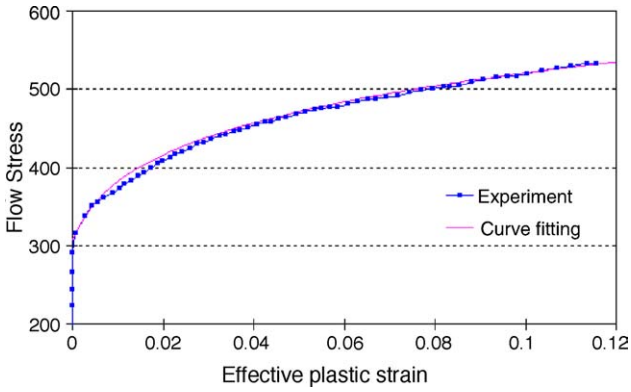

Fig. 4. Stress–strain relation obtained from tube expansion test.

Table 2
Summary of results obtained from experiment and FEM simulations[a]

No. of ball-segments	Parameters		Measurement	FEM
Three ball-segments	Thickness (mm)	Maximum	2.19	2.39
		Minimum	1.41	1.49
	Thickness change (%)	Thickening	15.3	25.8
		Thinning	25.8	21.6
	Axial strain	Maximum	0.3	0.27
		Minimum	−0.2	−0.24
	Hoop strain	Maximum	0.05	0.06
		Minimum	−0.02	−0.06

[a] Circular tube: R_b = 139.7 mm, o.d. = 69.85 mm, t_o = 1.9 mm.

stress–strain relation. Its constitutive equation is:

$$\sigma(\varepsilon_p) = K(\varepsilon_e + \varepsilon_p)^n \quad (1)$$

where K is the strength coefficient (732 MPa), ε_e the offset elastic strain (0.3%), n the work-hardening exponent (0.15), and ε_p is the effective plastic strain. For the elastic properties, the Young's modulus (E) of 206 GPa and Poisson's ratio of 0.3 were used in the simulations.

The only experimental data that were available for the bending of the steel was circular cross-sectioned tubes bent using a three ball-segment mandrel. To establish the reliability of FEM for rotary draw bending, a model for the experimental bending was performed. Table 2 summarizes the FEM results obtained compared to the experimental results. While the maximum wall thickness of the 90° bent circular tube by FEM simulation is overestimated by 0.2 mm, the minimum wall thickness on the outer wall has relatively good agreement with that from the experimental results. When bending with a three ball-segment mandrel, more than 20% wall thinning is observed and predicted. The overall comparison of the FEM results with the experimental results provides evidence that the present FEM bending model is a valid for simulations of the rotary draw bending process.

3. Results and discussion of FEM simulations

For a small tube diameter to thickness ratio, also known as the wall factor, it is feasible to bend the tube without a mandrel and not have major degradation in product quality. However, a mandrel in the bending operation is indispensable for most tubes to be used in hydroforming applications where the tube diameters are larger. The mandrel helps maintain tube shape during bending. The use of a mandrel deters wrinkling on the inside of the bend, as well as flattening or collapse on the outside of bend during the bending operation; however, thinning on the outside of the bend can become worse. It has been reported that for a circular cross sectional tube with a bend radius of two times the tube diameter and a wall factor of 31.8, the thinning ratio for bending with a mandrel is approximately 6.5% greater than without the mandrel [3].

Without a mandrel, the tube cross-section at the bend can collapse or experience hoop-buckling during the bending operation. Fig. 5 shows such situations. A bent circular tube (γ = 1.0) with R_b = 175.0 mm, t_o = 2.0 mm is shown in Fig. 5(a), in which β, the side-bulge parameter, equals the increase in diameter in the direction of the minor axis, and δ, the flattening parameter, equals the decrease in the length of the major axis. When the cross section of the tube is no longer convex, δ is a measure of the hoop-buckle. For example, in Fig. 5(a), the hoop-buckle and the side-bulge are quantified by δ = 22.42 mm and β = 1.00 mm, respectively.

In general, a bent tube, even with undesired deformation, can be used for hydroforming applications; however, most applications require the pre-formed tube to fit into the hydroforming dies, to guarantee the proper geometry and to maintain sufficient clearance. Because the pre-forming dies press on the undesired cross section, it can collapse even further. In such a case, even very high internal pressure during the hydroforming process may not be adequate to deform the tube so that it fills the final die cavity.

3.1. Flattening and hoop-buckling

When an oval tube with γ = 0.5 is bent under the same bending conditions as the circular tube shown in Fig. 5(a), the outside of the bend is not hoop-buckled, but just flattened (δ = 5.35 mm). The amount of the side-bulge is small (β = 0.31 mm) as seen in Fig. 5(b).

Fig. 6 shows the flattening-to-bend radius ratio (δ/R_b) along the bend as a function of angular position along the bend as measured from the tangent-line for tubes with the same aspect ratio (γ = 0.5) and wall thickness (t_o = 2.0 mm). As the bend radius increases, the maximum value of δ/R_b decreases. A power function fit to the maximum value points yields $\delta/R_b|_{max} = 5430.8R_b^{-2.34}$. The flattening along the bend tends to be constant. Table 3 summarizes the conditions when hoop-buckles occur for aspect ratios greater than γ = 0.5 with the same bend angle (θ_b = 90°) and wall thickness (t_o = 2.0 mm).

The maximum flattening distance measured along the outside of the bend is defined as δ_{max} regardless of whether hoop-buckling occurs or not. Fig. 7 presents the maximum amount of flattening (δ_{max}) predicted in tubes with constant bend radius (R_b = 175 mm). A line divides the hoop-buckled region

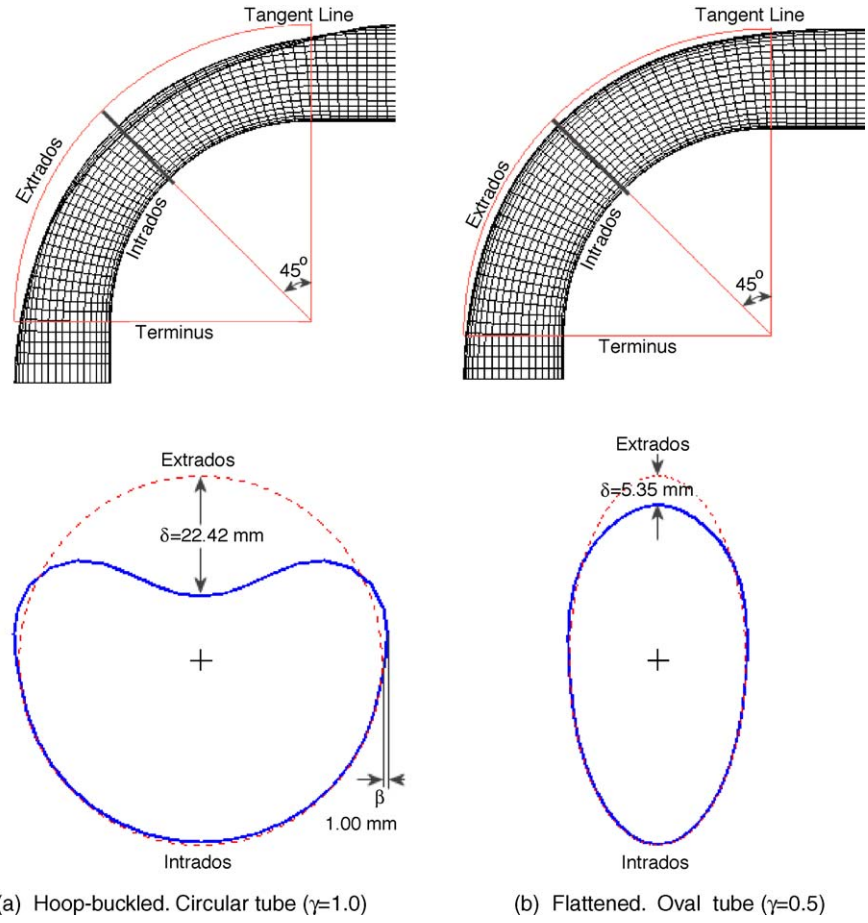

Fig. 5. 90° bent tubes and their cross sectional shapes for $R_b = 175$ mm and $t_o = 2.0$ mm: (a) hoop-buckled. Circular tube ($\gamma = 1.0$); (b) flattened. Oval tube ($\gamma = 0.5$).

from the region with only flattening. The hoop-buckled cases are marked with open symbols in the figure. All of the circular tubes hoop-buckled because the unsupported bend of the circular tube did not have sufficient stiffness to withstand the hoop stresses. However, most of the oval tubes are flattened without hoop-buckling. As the wall thickness of the oval tubes increases, the severity of hoop-buckling decreases and the value of δ_{max} decreases.

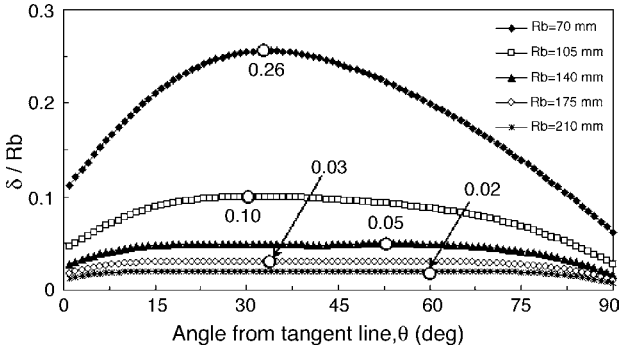

Fig. 6. Non-dimensional δ/R_b as a function of angular position along the bend (θ) measured from the tangent line for $\theta_b = 90°$, $\gamma = 0.5$ and $t_o = 2.0$ mm. (δ: extrados flattening, R_b: bend radius).

3.2. Side-bulge

A significant amount of the side-bulge in the bent tube can interfere with the closing of the hydroforming dies. An oval tube with less side-bulge is preferable for tubular hydroforming applications. Fig. 8 shows the maximum amount of side-bulge (β_{max}) observed in tubes with $R_b = 175$ mm. β_{max} is defined as shown in this figure. For oval tubes, as the wall thickness increases, the value of β_{max} decreases dramatically. As the aspect ratio for the oval shaped tube approaches a circle, β_{max} becomes larger. The small value of $\beta_{max} = 0.35$ mm for the circular tube with $t_o = 1.5$ mm and marked with (⋆)

Table 3
Occurrence of hoop-buckles for $\theta_b = 90°$ and $t_o = 2.0$ mm

R_b (mm)	$\gamma = 0.6$	$\gamma = 0.7$	$\gamma = 0.8$
70	Hoop-buckled	Hoop-buckled	Hoop-buckled
105	Hoop-buckle Initiated	Hoop-buckled	Hoop-buckled
140	Flattened	Hoop-buckle Initiated	Hoop-buckled
175	Flattened	Flattened	Hoop-buckle Initiated
210	Flattened	Flattened	Flattened

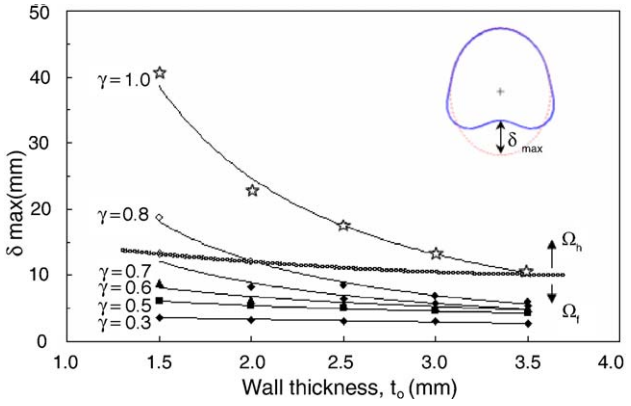

Fig. 7. Maximum amount of flattening (δ_{max}) as a function of the wall thickness with R_b = 175 mm. (Ω_f: flattened region without hoop-buckle, Ω_h: hoop-buckled region).

in Fig. 8 is somewhat deceptive. This lower value of β_{max} is because the hoop-buckling of the tube has reduced the measured value of side-bulge. In spite of the small value for side-bulge such a tube would be undesirable for subsequent hydroforming due to the hoop-buckling.

3.3. Wall thinning

Fig. 9 shows the thickness variation along the outside of the bend as the wall thickness varies in oval tubes with R_b = 175 mm and γ = 0.5. Points that indicate the thinnest wall thickness are marked with (☆) in the figure. The thinnest point in the wall is located at an angle of approximately 68° from the tangent line.

The minimum thinning ratio (ξ_{min}) is defined as:

$$\xi_{min} = \frac{t_o - t_{min}}{t_o} \times 100 \quad (2)$$

where t_o is the initial wall thickness, and t_{min} is the minimum wall thickness along the outside of the bend. As the initial tube wall thickness increases, the thickness variation increases, but the thinning ratio as defined by Eq. (2) remains below 12%.

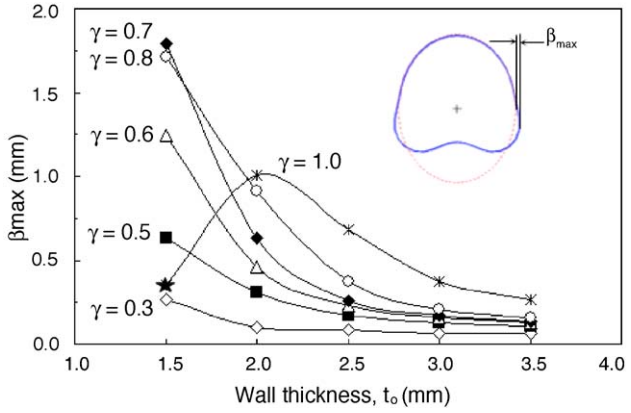

Fig. 8. Maximum amount of side-bulge (β_{max}) as a function of the wall thickness with R_b = 175 mm.

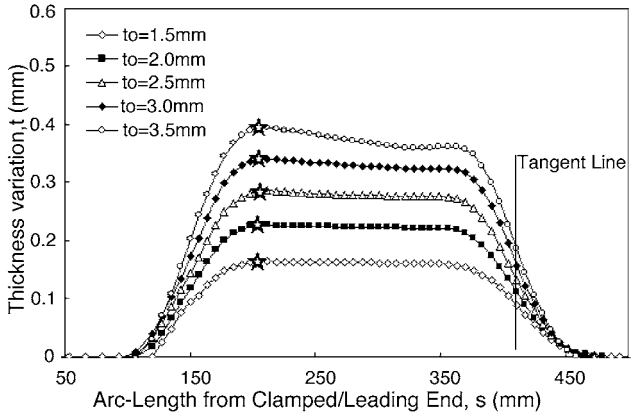

Fig. 9. Thickness variation along the outside of the bend for R_b = 175 mm and γ = 0.5 (☆ indicates the thinnest wall thickness).

Furthermore, when the tube wall is thick, such as t_o = 3.0 or 3.5 mm, the thickness variation tends to increase slightly with distance from the tangent line at the terminus of the bend.

For R_b = 175 mm, Fig. 10 shows minimum thinning ratios occurring on the outside of the bend, as the aspect ratio and the wall thickness vary. Due to more inward material collapse on the bend to minimize the strain energy in the tube, the overall thinning ratios decrease as the oval shape becomes closer to the circular one. However, the thinning ratio at γ = 0.3 is observed to be slightly smaller than that at γ = 0.5, which suggests that a tube with a cross section less than γ = 0.5 thins less. The smaller amount of thinning is due to the smaller amount of flattening. For γ = 0.3, as the wall thickness increases, the thinning ratio decreases linearly. However, for γ > 0.5, the thinning ratio increases as the wall thickness increases. Based on the observation in Fig. 7, hoop-buckling occurs in tubes with R_b = 175 mm, when the thinning ratio

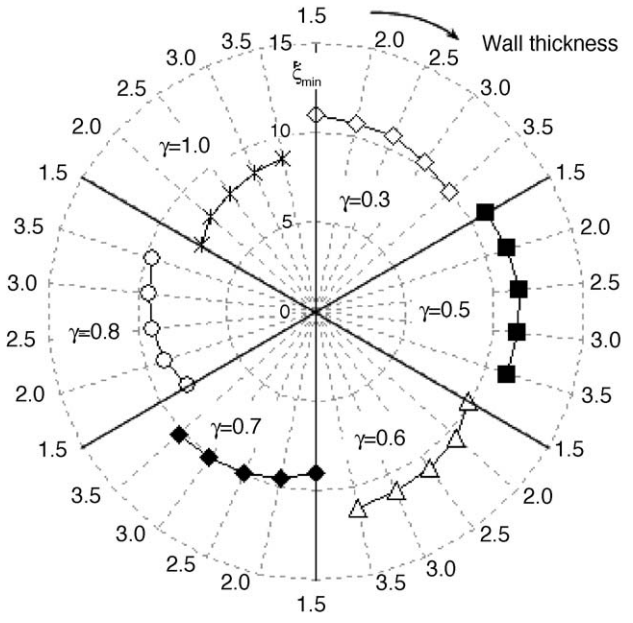

Fig. 10. Minimum thinning ratio on the outside of the bend for R_b = 175 mm.

is less than 9.1%. Although the thinning ratios of all the circular tubes are less than 8.7% and are the lowest compared with other oval tubes, they may not be applicable to current hydroforming applications due to the excessive hoop-buckle or the large amount of flattening.

3.4. Shape degradation factor

To interpret the data obtained from the finite element analysis, a factor, which aggregates the effects of various process parameters shown in Table 1, is defined. This factor called the 'shape degradation factor' (W), is

$$W = \frac{I_z}{(R_b t_o)^2} \tag{3}$$

where R_b is the bend radius, t_o the wall thickness, and I_z is the area moment of inertia for the cross section of the tube. I_z, is defined as

$$I_z = \frac{\pi}{4}(a_o^3 b_o - a_i^3 b_i) \tag{4}$$

where a_o, b_o, a_i, and b_i are shown in Fig. 11.

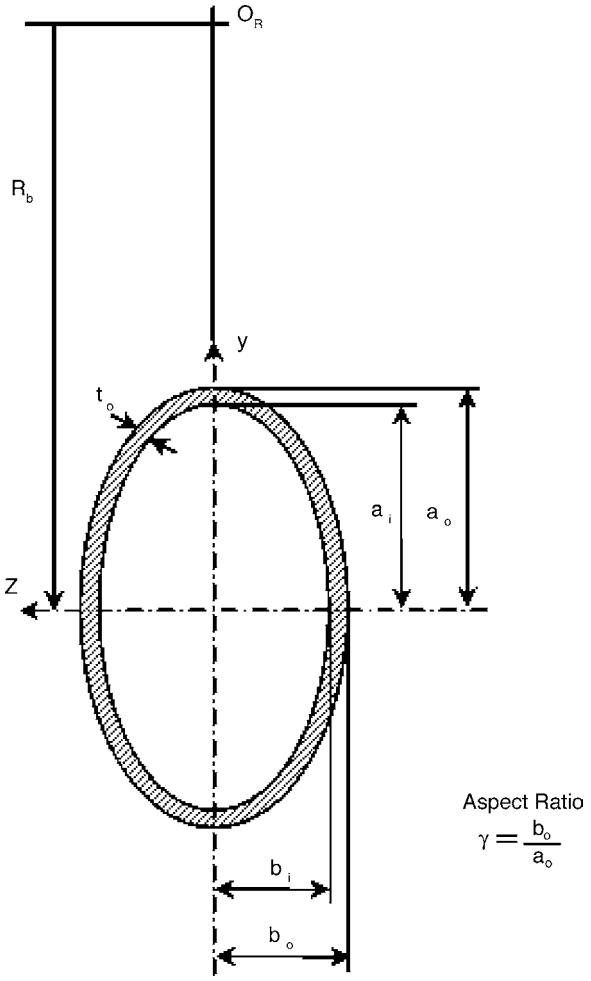

Fig. 11. Geometrical parameters of the cross section.

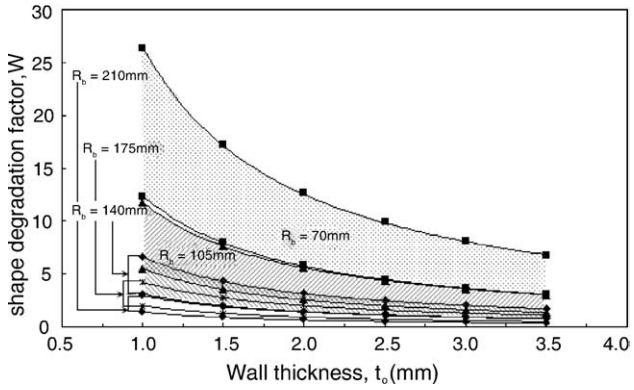

Fig. 12. Ranges of the calculated shape degradation factor for each bend radius.

The shape degradation factor, W, only applies to the hard-way bending, and it represents a degree of difficulty in producing high quality bent tubes. The cross-sectional shape, especially on the outside of the bend, will be more distorted inward as W increases. The closer to a circular cross section, i.e. the larger I_z becomes, the more flattening or hoop-buckling is observed. Hence, W is proportional to I_z. On the other hand, since a larger R_b and a thicker t_o help avoid undesired deformation, W is inversely proportional to R_b and t_o. By squaring the product of R_b and t_o in Eq. (3), W becomes dimensionless quantity. Calculated ranges of W based on Table 1 are shown in Fig. 12 for each bend radius. As the bend radius and the wall thickness increase, W decreases.

Based on the observations for all deformed cross sectional shapes for a 90° bend, hoop-buckle limits shown in Fig. 13 are found for each bend radius. The aspect ratio γ is not constant in determining the limits for each bend radius. While the shaded regions indicate that only flattening takes place in tubes, the non-shaded regions indicate the occurrence of hoop-buckling. For example, with $R_b = 105$ mm and $t_o = 1.5$ mm, two cases, i.e. P and Q, can be compared to see whether tubes at these points experience hoop-buckling. The shape degradation factor at point P is $W_P = 5.88$ and $W_Q = 4.71$ at point Q. The values of W are calculated for

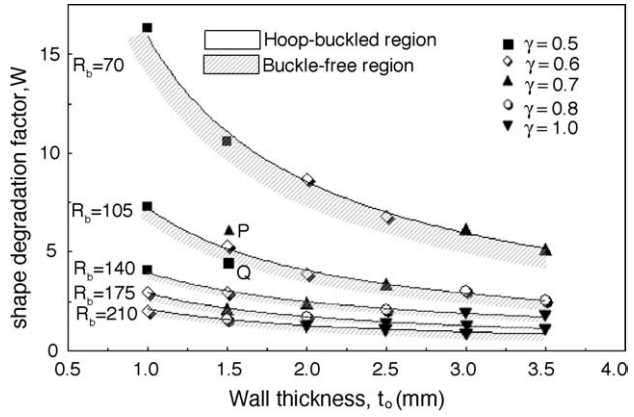

Fig. 13. Hoop-buckle limit diagram.

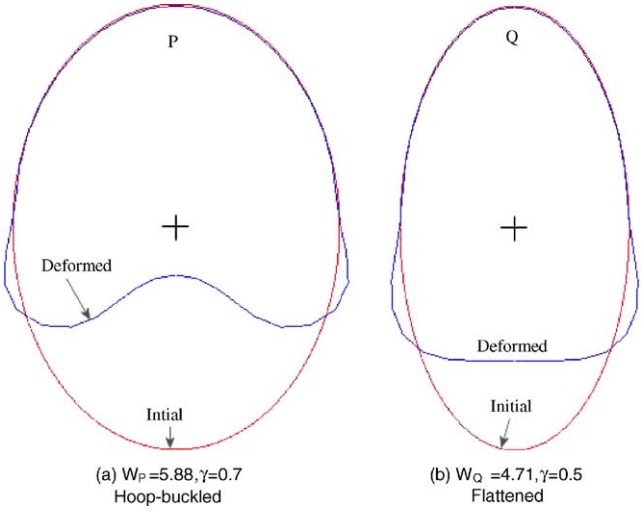

Fig. 14. Deformed cross sectional shapes at point P and Q for R_b = 105mm, t_o = 1.5 mm.

different aspect ratios but with similar bending conditions. Fig. 14 shows the deformed cross-sectional shapes at point P and Q. Hoop-buckling occurs at point P, but not at point Q.

To evaluate maximum flattening, Δ_{max}, data from the simulations excluding hoop-buckled cases are analyzed. Δ_{max} is the maximum value among the flattened values measured along the 90° bend. Fig. 15 shows the distribution of Δ_{max} as a function of the shape degradation factor W. Since all data from tubes with $\gamma = 0.3$ and a few having $\gamma = 0.5$ under the bend radius greater than 175 mm lie below the trend curve, less flattening occurs in those tubes for the same shape degradation factor. Furthermore, Fig. 15 shows that as the bend radius and the wall thickness decrease, the amount of Δ_{max} increases.

3.5. Acceptability criteria

Based on appropriate limits for flattening and side-bulge in 90° bent tubes, Table 4 and Fig. 16 suggest acceptability criteria for bending oval tubes suitable for tubular hydroforming applications without the need for a pre-forming step.

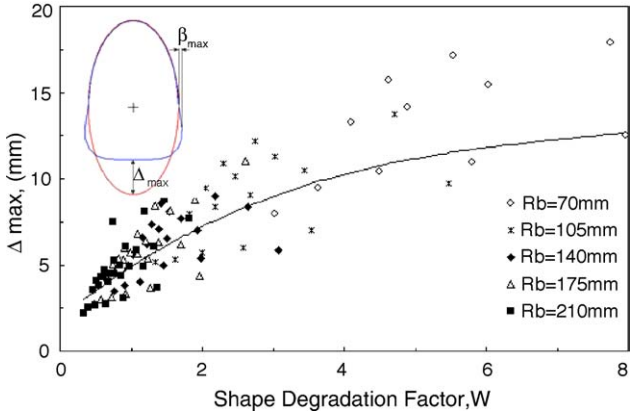

Fig. 15. Distribution of a newly defined flattening (Δ_{max}) as a function of shape degradation factor (W).

Table 4
Oval tube acceptability criteria for tubular hydroforming applications

Criterion	Maximum flattening (mm)	Maximum side-bulge (mm)
Not acceptable	$10 < \Delta_{max}$	$1.00 < \beta_{max}$
Restrictively acceptable	$8 < \Delta_{max} \leq 10$	$0.50 < \beta_{max} \leq 1.00$
Acceptable	$5 < \Delta_{max} \leq 8$	$0.25 < \beta_{max} \leq 0.50$
Very acceptable	$\Delta_{max} \leq 5$	$\beta_{max} \leq 0.25$

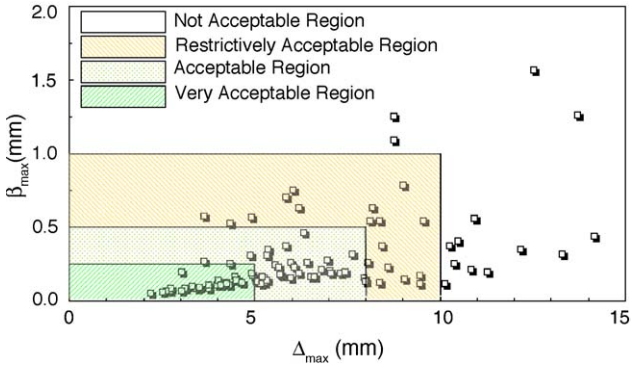

Fig. 16. Oval tube acceptability criteria for tubular hydroforming applications.

Based on the suggested acceptability criterion, regions for a suitable tubular hydroforming application are plotted in Fig. 17. Only a few cases with wall thickness equal to 1.0 mm can meet the "acceptable" criterion, due to insufficient geometrical rigidity to the material stretching on the outside of the bend. Most cases with t_o = 1.0 mm are severely flattened, hoop-buckled, or wrinkled on the bend. Tubes have difficulty meeting the "very acceptable" criterion, unless R_b is 2.5 times greater than the length of the major axis or γ is less than or equal to 0.5. The overlapped region in Fig. 17 can be considered a transient region, where the acceptability is dependent on the tube size and the bending conditions. For instance, the shape degradation factor, W_A at point A, shown in Fig. 17 is 1.45, which corresponds to R_b = 140 mm, $\gamma = 0.3$, and is 0.21 larger than W_B at point B, which corresponds to R_b = 175 mm, and $\gamma = 0.5$. Even though W_B is smaller than W_A, $\Delta_{max,A}$ is 4.99 mm and is smaller than $\Delta_{max,B}$ which is

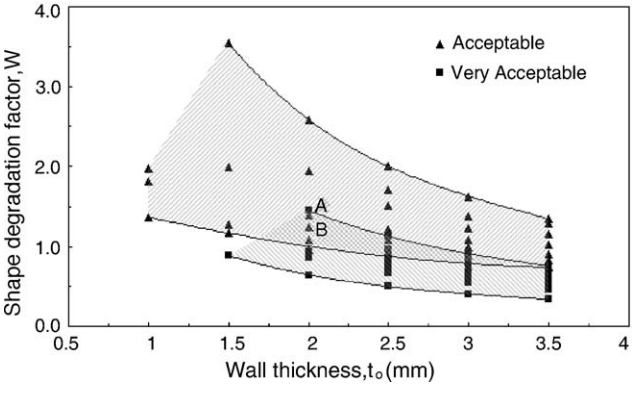

Fig. 17. Suggested acceptable regions of oval tubes for a suitable tubular hydroforming applications.

approximately 5.35 mm. Nevertheless, point B belongs in the "acceptable" region. Therefore, when a given bending condition lies in the transient region, the acceptability cannot be explicitly determined.

4. Summary

In this study, finite element modeling of the rotary draw bending process without the use of a mandrel was performed to gain insights and to examine the deformation characteristics of oval tubes. Bend radius, aspect ratio of the tube ovalness, and wall thickness were the major parameters investigated. For all simulations, the length of the major axis on the oval cross section equals 70.0 mm, and all tubes were bent up to 90° with the hard-way bend. The Coulomb friction model with 0.1 friction coefficient was used in the simulations.

In spite of the relatively low thinning ratio compared with oval tubes, circular cross-sectional tubes used in automotive hydroforming applications often collapse or hoop-buckle if a mandrel is not used during the bending operation. This undesirable cross-sectional shape is squeezed in a pre-forming operation and further collapse can occur. In such cases, higher internal pressure during the hydroforming cannot deform the tube so that it fills the final die cavity. However, proper selection of oval tubes for a given bending condition helps improves the shape of the bent tube because hoop-buckling or wrinkling on the bend can be avoided even though a mandrel is not employed. Bending of oval tubes rather than circular ones reduces both wall thinning (5–10%) and strain (7–20%) on the outside of the bend when compared to circular tubes bent with the aid of a mandrel. It is observed that an oval tube tends to be easily hoop-buckled or excessively flattened (1) as it approaches a circular cross section, (2) as the bend radius becomes smaller, and (3) as the wall thickness becomes thinner. The maximum side-bulge on the bend decreases as the wall thickness and the bend radius increase and the aspect ratio decreases.

In order to represent the degradation of the cross-sectional shape, a non-dimensional shape degradation factor was defined as a function of area moment of inertia, bend radius, and wall thickness. It is only valid for the hard-way bend of an oval tube. Observations were made to find a hoop-buckle limit diagram in terms of the shape degradation factor. For hoop-buckled oval tubes, the use of a mandrel may improve the shaping quality, and a booster system can reduce wall thinning or strain along the outside of the bend.

A reasonable criterion for oval tubes is suggested by limiting both the maximum flattening and the side-bulge. Acceptable regions are found even though a small amount of flattening or side-bulge takes place. For bending applications requiring a tight bend or where minimal wall thinning is required, not only flattening and side-bulge, but also wall thinning and strain need to be properly considered.

Acknowledgements

The authors express their appreciation to POSCO, which has supported the graduate study of the lead author within the Advanced Steel Processing and Products Research Center at Colorado School of Mines (CSM). We also acknowledge the helpful discussions of this work with Profs. B.S. Levy and M.T. Lusk of CSM and Dr. R. Stevenson of GM Research.

References

[1] M. Koç, T. Altan, An overall review of the tube hydroforming (THF) technology, J. Mater. Process. Technol. 108 (2001) 384–393.
[2] K. Manabe, M. Amino, Effects of process parameters and material properties on deformation process in tube hydroforming, J. Mater. Process. Technol. 123 (2002) 285–291.
[3] H. Singh, Computer simulation of tubular hydroformng, Tube Pipe J. 11 (2000) 8–13, March.
[4] N. Rodriguez, D. Schlatter, Contribution of a booster device on tube rotary draw bending: experimental and finite element analysis, Stainless Steel 1999 Science and Market, Third European Congress (Italy), vol. 2, June 1999. pp. 229–236.
[5] J.B. Yang, B.H. Jeon, S.I. Oh, The tube bending technology of a hydroforming process for an automotive part, J. Mater. Process. Technol. 111 (2001) 175–181.
[6] S.G. Shr, Bending of Tubes for Hydroforming: A State-of-the-Art Review and Analysis, MS Thesis, Ohio State University, Columbus, OH, USA, 1998.
[7] M. Sukimoto, Y. Taguchi, M. Sakaguchi, H. Akiyoshi, J. Endou, Deformation of a cross section of 6063 alloy circular tube by rotary draw bending, J. Jpn. Inst. Light Met. 44 (1994) 475–479.
[8] F. Costello, D.J. DeWitt, Tooling functions in rotary draw bending: reviewing the basic equipment, The Fabricator 24 (June 5) (1994) 28–31.
[9] R.R. Stange, Tooling and methods for tube and pipe bending: the importance of proper equipment and proven techniques, Tube Pipe J. (1997) 28–35, Nov/Dec.
[10] P.R. Bevington, D.K. Robinson, Data Reduction and Error Analysis for the Physical Sciences, second ed., McGraw-Hill, New York, NY, USA, 1992.